Journal of Crohn's and Colitis, 2017, 1247–1257
doi:10.1093/ecco-jcc/jjx075
Advance Access publication May 27, 2017
Original Article

Original Article

Genetic Mouse Models with Intestinal-Specific Tight Junction Deletion Resemble an Ulcerative Colitis Phenotype

Wolfgang Stremmel[a], Simone Staffer[a], Mathias Jochen Schneider[b], Hongying Gan-Schreier[a], Andreas Wannhoff[a], Nicole Stuhrmann[a], Annika Gauss[a], Hartwig Wolburg[c], Anne Mahringer[d], Alexander Swidsinski[e], Thomas Efferth[b]

[a]Department of Internal Medicine IV, University Clinics of Heidelberg, Heidelberg, Germany [b]Department of Pharmaceutical Biology, Institute of Pharmacy and Biochemistry, Mainz, Germany [c]Department of Pathology and Neuropathology, University Medical School of Tübingen, Tübingen, Germany [d]Institute of Pharmacy and Molecular Biotechnology, Ruprecht-Karls-University of Heidelberg, Heidelberg, Germany [e]Department of Gastroenterology, University Hospital Charité of Berlin, 10115 Berlin, Germany

Corresponding author: Wolfgang Stremmel, MD, PhD, Professor of Medicine, University Clinics of Heidelberg, Department of Internal Medicine IV, 69120 Heidelberg, Germany. Tel: +49 6221 56 8700; Email: wolfgang.stremmel@med.uni-heidelberg.de

Abstract

Background and Aims: A key pathogenetic feature of ulcerative colitis [UC] is an intrinsic low mucus phosphatidylcholine[PC] content. Recently, a paracellular transport for PC across tight junctions[TJs] was described, suggesting TJ disturbance as a cause of diminished luminal PC transport. Therefore, we aimed to generate mutant mice with TJ deletion to evaluate whether a UC phenotype developed.

Methods: CL57BL/6 control wild-type mice were compared to mutant mice with tamoxifen-induced villin-Cre-dependent intestinal deletion of kindlin 1 and 2.

Results: Electron microscopy of mucosal biopsies obtained from both mutants before overt inflammation following only 2 days of tamoxifen exposure revealed a defective TJ morphology with extended paracellular space and, by light microscopy, expanded mucosal crypt lumina. PC secretion into mucus was reduced by >65% and the mucus PC content dropped by >50%, causing a >50 % decrease of mucus hydrophobicity in both mutants. Consequently, the microbiota was able to penetrate the submucosa. After 3 days of tamoxifen exposure, intestinal inflammation was present in both mutants, with loose bloody stools as well as macroscopic and histological features of colitis. Oral PC supplementation was able to suppress inflammation. By analogy, colonic biopsies obtained from patients with UC in remission also showed a defective epithelium with widened intercellular clefts, and enlarged crypt luminal diameters with functionally impaired luminal PC secretion.

Conclusions: Genetic mouse models with intestinal deletion of kindlin 1 and 2 resulted in TJ deletion and revealed pathophysiological features of impaired PC secretion to the mucus leading to mucosal inflammation compatible with human UC.

Key Words: Mucosal barrier; mucus; phosphatidylcholine; hydrophobicity; ulcerative colitis

1. Introduction

Ulcerative colitis [UC] is an inflammatory bowel disease characterized mostly by bleeding and diarrhoea. Contemporary therapies focus on anti-inflammatory strategies.

The pathogenesis of UC is unknown. The traditional view is that a primary deregulation or overactivation of the gut immune system, e.g. the T cells, is responsible. An alternative view proposes as the underlying cause a defective mucosal barrier which, after bacterial invasion, may secondarily activate the immune system.[1]

Mucus hydrophobicity as a key component of the mucosal barrier is established by the phosphatidylcholine [PC] content therein.[2] The fact that >90% of the phospholipids in mucus are represented by PC species[3] suggests that they are actively transported there. In animal studies, it was shown that PC is predominantly secreted into the ileal mucus and only marginally in the colon,[4] which is probably due to the significantly higher surface area in the ileum and not to an intrinsic PC secretory defect in colon. This is remarkable because the mucus barrier shield is most needed in colon, where it faces one trillion bacteria per gram of stool. It was therefore proposed that the PC secreted in the ileum moves to the colon to provide sufficient protection.[5]

At the molecular level, it was recently shown that the apical transport of PC into the mucus compartment occurs along a newly described unique paracellular route between mucosal epithelial cells and across tight junctions [TJs].[6] PC transport is stimulated by an electrochemical gradient with apical accumulation of negative charge through the cystic fibrosis transmembrane conductance regulator [CFTR].[6] After translocation across the TJ complex, PC is first bound to membrane-associated mucin 3, from where it is handled to secretory mucin 2.[6,7] The PC–mucin 2 complex is capable of moving within the mucus distally along the colonic wall to the rectum. During this transport to the rectum, mucus PC can be broken down by ectophospholipases of the commensal bacterial flora similarly as was shown for *Helicobacter pylori* in the gastric mucosa.[8] This means that the hydrophobic mucus PC shield is lowest in the rectum, and that is where the mucosa is most vulnerable to infection.

It was surprising to see that rectal mucus of UC patients in remission – but not Crohn's disease patients – revealed a 70% reduction of its PC content.[9,10] This finding indicates that decreased PC is intrinsic to UC. The resulting reduced mucus hydrophobicity[11] allows for invasion by colonic microbiota and subsequent inflammation that begins in the rectum and extends proximally according to the degree of PC depletion and the corresponding mucosal vulnerability.

The observation that PC is predominantly secreted by the ileal mucosa – which is impaired in UC – may explain the phenomenon of backwash ileitis in cases of pancolitis where opening of the ileocecal valve allows higher microbiota exposure to a potentially more vulnerable terminal ileum mucosa. Moreover, it also explains the phenomenon that pouchitis – the inflammation of an ileal reservoir – occurs only in patients after colectomy for UC, and never in pouches of patients with familial adenomatous polyposis [FAP].

To support the idea that UC is caused by diminished paracellular transport of PC to the intestinal lumen, we generated mouse models with intestine-specific deletion of kindlin 1 and 2, which, among other functions, activate integrins and serve cell adhesion to the basal membrane or at cell-to-cell junctions, respectively[12–15]. Due to a higher biological priority of basal attachment it was assumed that in case of kindlin 1 deletion, kindlin 2 translocates from the lateral to the basal membrane, and secondarily impairs cell-to-cell adhesion. Moreover, adherence and tight junctions are closely connected.[16–18] Thus, the loss of adherence junctions finally impairs TJs, which causes disturbed paracellular PC translocation to the luminal side of mucosal cells.[6]

In fact, constitutive kindlin $1^{(-/-)}$ mice have been reported to develop a severe UC phenotype during the neonatal period.[15] Kindlin $2^{(-/-)}$ mice, however, experience embryonic death.[14] Therefore, in this study, we chose time- and tissue-selective conditional knockout mice models with tamoxifen-sensitive, intestinal-specific kindlin 1 or 2 deletion for evaluation of the initiating events leading finally to an adult UC phenotype. The pathogenetic features of defective PC secretion into mucus and its pathophysiological consequences were analysed. The results were compared to biopsies from patients with UC in complete remission, Crohn's disease and control subjects.

2. Material and Methods

2.1. Characterization of the UC phenotype in genetic mouse models and human subjects

Animal studies followed the 'ARRIVE' guidelines and were approved by the Heidelberg ethics committee [Ref-# 35-9185.81/6123/10 and 6284/11] as well as the acquisition of human biopsy samples [Ref-# S-211/2010]. Male C57BL/6 wild-type mice were obtained from Charles River. The corresponding tamoxifen-inducible, villin-Cre-dependent, kindlin 1 and 2 intestine-specific knockout mice were gifts from R. Faessler[13–15] and propagated after embryonic transfer in the animal facilities of the University of Heidelberg. Wild-type and mutant mice were co-housed in the sense that wild-type mice and kindlin $1^{(-/-)}$ and $2^{(-/-)}$ mice were kept under identical breeding conditions in the same environment. They received LasVendi Rod 18 complete diet [Soest] *ad libitum* and were kept in conventional caging with ABBEDD LT-E-001 bedding at 22 °C, with a 12/12-h light/dark cycle. Control wild-type and mutant mice [12-week-old mice with a comparable body weight of 31 ± 2 g] were intraperitoneally [i.p.] injected at 9:00 a.m. with 0.2 mg tamoxifen daily for up to 3 days before being killed 1 day later. Ileal mucosal cells were isolated[19] and characterized by western blotting using antibodies to mouse kindlin 1 and 2, ZO1, occludin, claudin2 and β actin as previously described[6] as well as to total integrin ß1 [N-20, sc-6622, 1:200; Santa Cruz]; activated integrin ß1 [553715; 1:1000; BD Pharmingen]; e-cadherin [36/E, 610181, 1:2500; BD Transduction Bioscience]; claudin 2 [3F1, sc-293233, 1:200; Santa Cruz]; and occludin [EPR8208, ab167161, 1:100; Abcam].

The UC phenotype was assessed after 3 days of tamoxifen exposure by endoscopy using a flexible Elite Visera LV-S190 laryngoscope [Olympus]. The ileum was chosen for endoscopy because it showed a similar inflammatory phenotype as the colon. Moreover, due to its wider lumen, it was more easily accessible by the employed endoscope after incision of the wall at the terminal ileum and proximally directed endoscopy. Indeed, colonoscopy from anus often resulted in perforation of the colonic wall. Quantitative evaluation of the UC phenotype was performed in resected gut segments and included the macroscopic colitis score with determination of the total colon weight [including stool content], length and stool appearance, as well as the histopathological colitis score after haematoxylin and eosin [HE] staining with determination of the extent of inflammation, crypt architecture, hyperaemia/oedema and immunocyte infiltration.[20] Histological assessment was performed by three independent investigators in a blinded manner. Furthermore, the calprotectin concentration in stool was determined as a marker of mucosal inflammation representing leukocyte accumulation in stool[21,22] using the S100A9/calprotectin, mouse, enzyme-linked immunosorbent assay (ELISA) kit [Hycult Biotech]. The same parameters were assessed

when the mutant mice were treated with 10 mg PC [P3556, Sigma] daily in 150 µl phosphate-buffered saline [PBS] by oral gavage during the 3 days of tamoxifen treatment[23] to assess improvement of the UC phenotype. Application by oral gavage – using a 6.5-cm 18G × 2-inch flexible elastic tube [9918, Cadence Science] – ensures that the full dose of PC is provided to the small intestine. The dosage of 10 mg PC per 100 ± 14 g mice body weight [100 mg/kg] was higher than the effective dose of 3.2 g delayed released PC used in previous human studies [corresponding to approximately 40 mg/kg].[24] This approach allows the absorption capacity of PC to be exceeded, and thus a significant amount of PC to enter unchanged into the distal intestine for subsequent incorporation into mucus. This process was not examined further in this study and we relied here on the published results.[23]

For functional analysis of the underlying mechanism leading to mucosal inflammation, mice were examined after 2 days of tamoxifen administration when the gross appearance of the mucosa was still intact [pre-inflammatory state], to avoid interference by a secondary inflammatory response. The mucus PC concentration in 5-cm sections of the distal ileum and colon [obtained by light scraping] was analysed by electrospray ionization MS/MS, focusing on the most abundant PC species with a mass of 36:2, which indicates 36 C atoms and two double bonds which corresponds to 18:0 and 18:2 fatty acid residues at the PC molecule.[25,26] This PC concentration was related to mucin 2 levels, determined by an in-house developed ELISA. Mucin 2 [M2378, Sigma] was used as a standard for calibration and an anti-mucin 2 antibody [B306.1/sc-59859, 1:100; Santa Cruz] was used for quantitative detection. *In vivo*, [^{3}H]PC recovery in the same intestinal mucus compartments was measured 16 h after intravenous injection of 10^{6} c.p.m. [^{3}H]PC, [^{14}C]inulin or [^{3}H]phosphatidylinositol [PI] [Perkin Elmer].[4]

Mucosal architectures and crypt lumen diameters were evaluated by light microscopy [Microscope Provis AX70, Olympus] in randomly selected HE-stained biopsy specimens obtained from 2-day tamoxifen-exposed wild-type or kindlin mutant mice [n = 6 each]. For human studies, colonic biopsies of control subjects, patients with UC in complete clinical, endoscopic and histological remission, or patients with Crohn's disease [n = 6 each] were evaluated. The ratios of the crypt lumen/total crypt diameter in at least 100 crypt sections of comparable size from similar locations were analysed independently by three investigators in a blinded manner. To determine the luminal phospholipid content, sections of the mouse ileum and human colon were stained with Pearse's reagent[27] [Electron Microscopy Science] or periodic acid-Schiff [PAS] stain [Merck]. Confocal laser microscopy[28] was used for analysis of paracellular PC movement. Ileal specimens of wild-type and mutant mice were subserosally injected with 200 µl of 10 µM nitrobenzo-oxa-diazole [NBD]-PC [Avanti Polar Lipids] in PBS and incubated for 1 h. The biopsies were snap-frozen in nitrogen slush [–210 °C] and sectioned in 6 µm slices. Furthermore, colonic mucosal biopsies of patients with UC in remission, Crohn's disease and normal controls were also incubated with 10 µM NBD-PC for 1 h under tissue culture conditions. For confocal laser microscopy, frozen sections were mounted in ProLong Diamond antifade reagent [ThermoFisher Scientific] and visualized on a Leica TCS SP 5 II confocal microscope [Leica Microsystems] using a 63.0 × 1.4 NA oil objective lens. NBD-PC was excited with the 458 nm and 488 nm lines of the argon laser and collected with a band-pass emission filter [504–545 nm]. A pinhole diameter of 1 Airy was used as default setting and a single optical image was captured by averaging eight pictures using the LAS AF software [Leica Application Suite Advanced Fluorescence Software] with 512 × 512 pixels and a standard 8-bit greyscale resolution. Brightness and contrast were adjusted likwise by Image J software [Image Processing and Analysis in Java, National Institute of Health].

For ultrathin section electron microscopy, intestinal probes were removed, fixed overnight in 2.5% glutaraldehyde [Paesel-Lorei] in 0.1 M cacodylate buffer [pH 7.4], postfixed in 1% O_sO_4 in 0.1 M cacodylate buffer for 1 h, dehydrated in an ascending series of ethanol and stained in uranyl-acetate-saturated 70% ethanol for 4 h. Dehydration was completed in propylene oxide. Finally, tissue was flat-embedded in Araldite [Serva]. Using an ultramicrotome [Ultracut, Leica], 50 nm sections were cut and stained with lead citrate, mounted on copper grids and finally analysed with a Zeiss EM 10 electron microscope. For freeze-fracture electron microscopy, the glutaraldehyde-fixed intestinal probes were cryoprotected in 30% glycerol and snap-frozen in nitrogen slush [–210°C]. Subsequently, they were fractured in a Balzer's freeze-fracture device [BAF400D; Balzers] and replicas were analysed with the Zeiss EM 10 transmission electron microscope.[29]

The mucus hydrophobicity measurements of the colonic mucosa were performed by goniometry [G1 Kruess Goniometer].[11] This technique determines the angle of a fluid drop on a given surface – here, the mucosa. The wider the contact angle, the higher the surface hydrophobicity. For the mucosa, it is mainly the PC content of the mucus which determines hydrophobicity. Fluorescence *in situ* hybridization [FISH] analysis of the ileal mucosa [30,31] was performed using a Nikon e600 fluorescence microscope [Nikon].

2.2. Statistical analyses

Statistical analysis was performed using Prism 4.0 software [GraphPad Software]. Differences between groups were evaluated using the Mann–Whitney U test. Multiple groups were compared by one-way analysis of variance [ANOVA] with a Dunnett's post-hoc test. Data are presented as means ± SD or medians with range, and $P < 0.05$ was considered statistically significant.

3. Results

3.1. Intestinally deleted kindlin 1 and 2 mice reveal disturbed TJs

It was proposed that PC as an essential component of the mucus passes from systemic sources along a paracellular route between enterocytes across the TJ barrier to the luminal side for incorporation into mucus.[6] Accordingly, the first challenge was to select an appropriate genetic mouse model with a distinct defect of TJs in the intestinal mucosa. Therefore, we chose adult mice with tamoxifen-inducible, villin-Cre-mediated intestinal deletion of kindlin 1 and 2, which are known activators of integrins.[13–15] Among other functions, they are responsible for cell adhesion and control of the apical TJ barrier.[12–18] Indeed, freeze-fracture electron microscopy[29] showed disturbed TJs which occurred in the pre-inflammatory state after 2 days of tamoxifen exposure of the mutant mice [Figure 1A]. In controls, epithelial TJs were arranged in a closely meshed network of strands, whereas in the mutants, the strands formed irregular blind endings. A more general morphometric light microscopy analysis of mucosal biopsies after HE staining revealed expansion of the mucosal crypt lumina in the mutants compared to controls [$P < 0.01$] [Figures 1B and 2A].

Higher resolution confocal laser microscopy revealed the cylindrical columnar and closely packed architecture of the normal wild-type mucosal cell lining was changed in mutants to a less organized epithelial layer with low cell density and extended paracellular spaces. In kindlin $1^{(-/-)}$ mice with a primary loss of basal attachment,

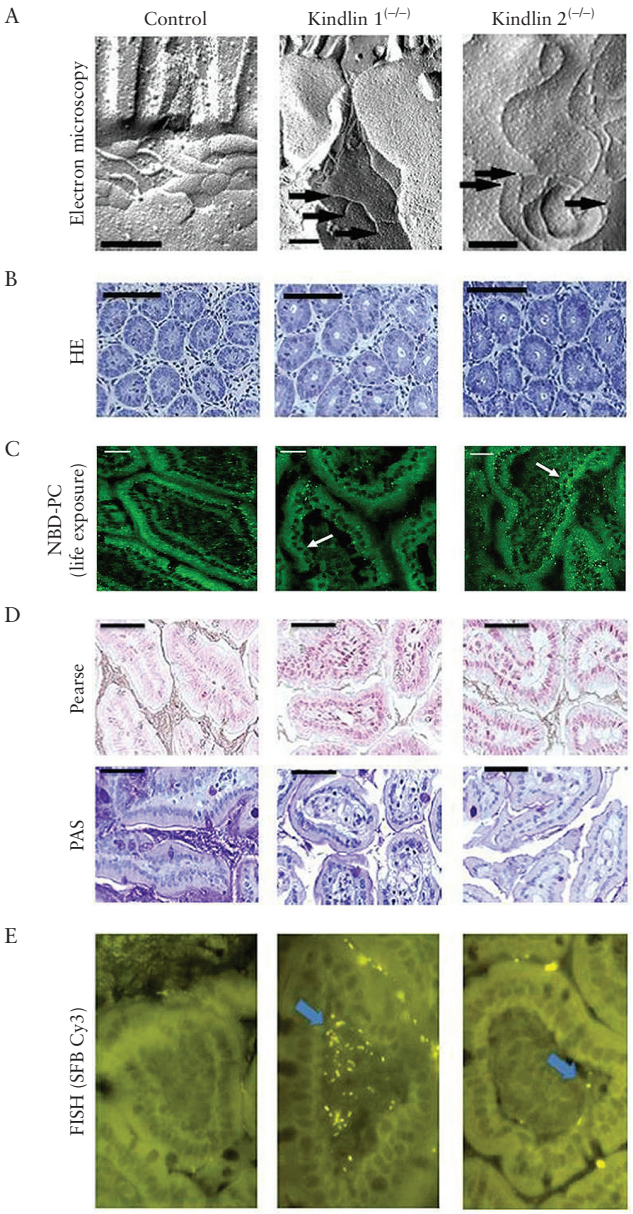

Figure 1. Pre-symptomatic features of ileal mucosa in the genetic mouse models of UC versus wild-type controls. [A] Electron micrographs of freeze-fracture replicas showing a close network of TJs in controls and TJ disturbance with open ends of the strands in the mutants [arrows mark open ends of TJ strands; scale bars = 0.2 µm]. [B] Widening of crypt diameters in mutants [HE staining]. [C] NBD-PC life exposure of ileal biopsies showing in controls a cylindrical, tightly packed arrangement of enterocytes with paracellular and mucus fluorescent staining. In mutants the cells are cuboidal with extended paracellular spaces and impaired PC staining, in particular of the mucus [cuboidal cells in kindlin $1^{(-/-)}$ and kindlin $2^{(-/-)}$ mice are indicated by white arrows]. [D] Reduced luminal Pearse and PAS phospholipid staining in mutants compared to controls [scale bars in B–D = 25 µm]. [E] FISH [1000-fold magnification] of segmented filamentous bacteria penetrating the ileal mucosa in mutants but not in controls.

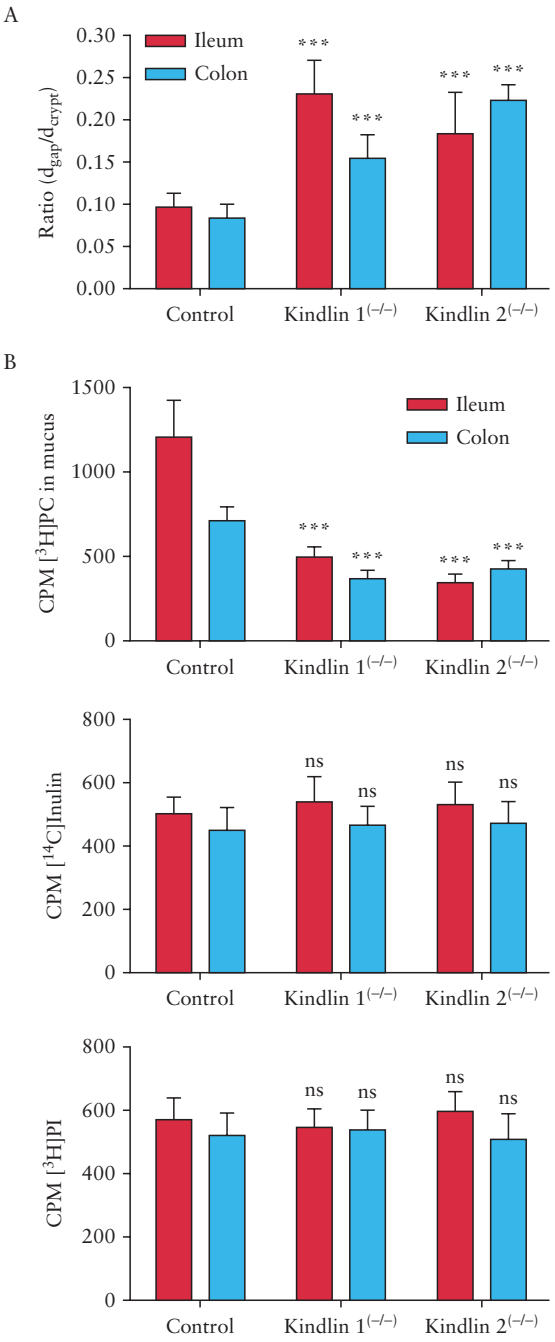

Figure 2. Crypt diameters and intestinal PC secretion capacity versus inulin and PI in control and mutant mice after 2 days of tamoxifen exposure [pre-inflammatroy state]. [A] Ratio of luminal diameter [^{d}gap] to total crypt diameter [^{d}crypt]. Colon: control, 0.084 ± 0.016; kindlin $1^{(-/-)}$, 0.155 ± 0.028; kindlin $2^{(-/-)}$, 0.223 ± 0.019. Ileum: control, 0.097 ± 0.016; kindlin $1^{(-/-)}$, 0.231 ± 0.040; kindlin $2^{(-/-)}$, 0.184 ± 0.049 [$P < 0.01$ mutants vs. controls] [$n = 6$]. [B] *In vivo*-determined secretion rates at 16 h after intravenous administration of substrates revealed suppression of mucus recovery of [^{3}H]PC in ileum and colon of kindlin $1^{(-/-)}$ and $2^{(-/-)}$ mice. The recovery rates of [^{14}C]inulin and [^{3}H]PI were unaltered [$n = 12$]. Means ± SD. ***$P < 0.01$; ns: not significant [mutants vs. controls].

the enterocytes were arranged in overlapping layers of the mucosal surface with an adopted cuboidal cell shape. In kindlin $2^{(-/-)}$ mice with a primary loss of cell adherence, enterocytes were also cuboidal, but remained within the mucosal cell lining [Figure 1C]. All these findings are consistent with the phenotype of disrupted TJs and loss of cell-to-cell adhesion. Western blot analysis of isolated mucosal cells in mutants revealed a decrease in representative proteins constituting the link from kindlins to integrin activation, to adherence junctions [e-cadherin] and finally to TJs [ZO1, occludin, claudin2] [Figure 3]. This supports the morphological findings and probably

indicates synthesis suppression of the involved proteins in mutants, which finally results in disruption of aged TJ bundles due to lack of renewal.

3.2. Functional implication of a disturbed TJ barrier

We next verified the hypothesis that TJs are responsible for the mucus PC accumulation. For functional analysis, the appearance of intravenously injected [^{3}H]PC in comparison to [^{14}C]inulin [as a cell-impermeable marker] and [^{3}H]PI [as another phospholipid] [all at 10^{6} c.p.m.] into the ileal and colonic lumen was examined *in vivo*. PC secretion was reduced in the mutants – most prominently in the ileum – by 60.3 ± 9.7% [$P < 0.01$]. The PC secretion of [^{14}C]inulin or [^{3}H]PI was intrinsically low and not altered between control and mutant mice [$P > 0.05$] [Figure 2B]. This indicates that at this early point in time only luminal PC secretion is impaired, whereas the mucosal barrier was otherwise functionally intact. PC transport after subserosal injection of NBD-PC was visualized by confocal laser microscopy. PC was only extracellularly detectable, in particular within the paracellular space between the enterocytes and in the mucus. In comparison to wild-type mice, staining in mutants was weaker and less prominent in the apical mucus. The data of disturbed lateral cell attachment and impaired PC secretion to mucus in mutants were compatible with our previous findings in the transwell tissue culture study employing polarized CaCo2 cells, which showed an apically directed paracellular and PC-specific secretion pathway, which was disrupted by

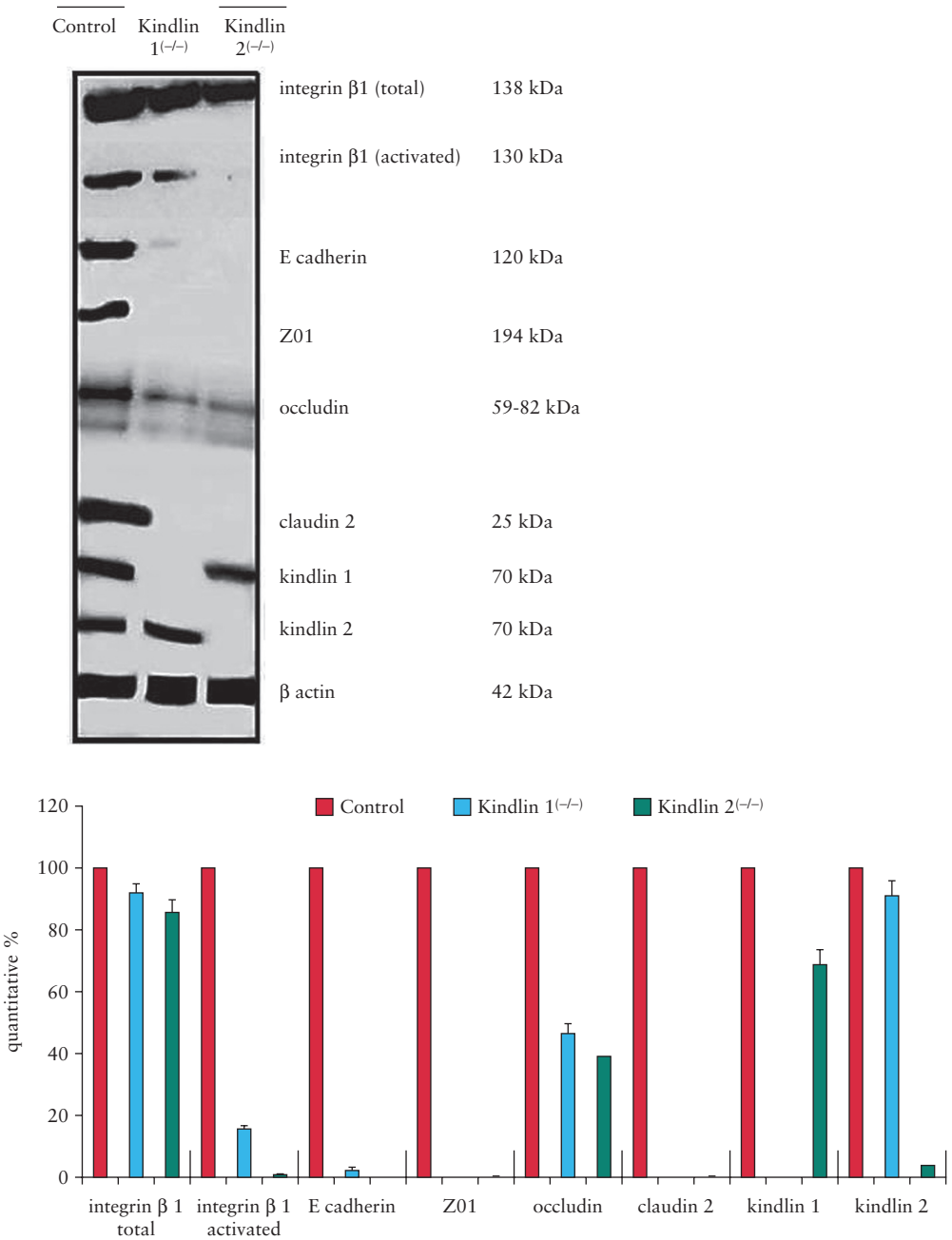

Figure 3. Western blot of isolated mucosal cells from control and mutant mice. Blots were stained with antibodies to proteins of the kindlin to β1-integrin activation to E-cadherin [adherence junction] and to representative TJ proteins [ZO1, occludin, claudin2].

knockdown of kindlin 1 or 2 as well as other TJ-associated proteins.[6] Accordingly, in the present study kindlin $1^{(-/-)}$ and $2^{(-/-)}$ mice showed a decreased PC content in the crypt lumen as detected by Pearse's stain[27] and PAS staining [Figure 1D]. Quantitatively, the ileal mucus PC concentration decreased from 80 ± 23 in controls to 39 ± 27 and 27 ± 19 nmol/mg mucin 2 in kindlin $1^{(-/-)}$ and $2^{(-/-)}$ mice, respectively [$P < 0.01$ for both mutants, $n = 6$]. This indicates that the PC load of mucin 2 is lower due to insufficient luminal PC secretion.

Lack of PC reduced the hydrophobicity of the mucus surface, as shown by contact angle goniometry. Values of 72 ± 6° in controls dropped to 30 ± 2° and 35 ± 1° in kindlin $1^{(-/-)}$ and $2^{(-/-)}$ mice, respectively [$P < 0.001$ for both mutants, $n = 6$]. Reduced hydrophobicity allowed for the penetration of microbiota into the submucosa. Accordingly, FISH[30] using the segmented filamentous bacterium Cy3 probe[31] confirmed only in mutant mice the submucosal penetration of microbiota, which activates the immune response[32] [Figure 1E].

3.3. Clinical impact of PC-depleted mucus

All of the above experiments describe the pathophysiological events of a compromised intestinal barrier function due to lack of mucus PC, although the gross appearance of the mucosa was still intact after 2 days of tamoxifen exposure [non-inflammatory state]. However, when the mutant mice were exposed to tamoxifen for 3 days, they consequently developed overt mucosal inflammation mimicking a UC-like phenotype in the ileum and colon [Figure 4], as was also observed in other genetic mouse models of inflammatory bowel diseases [IBDs].[33] The stool was soft, amorphic, sticky and contained blood. The oedema of the intestinal wall resulted in colonic weight gains of 202.2 ± 38.7% and 197.3 ± 37.2% and length reductions by 31.1 ± 6.7% and 32.3 ± 11.3% in kindlin $1^{(-/-)}$ and $2^{(-/-)}$ mice, respectively, versus control wild-type mice [$P < 0.01$ for both parameters in both mutants; $n = 6$; Figure 4 and Table 1]. In mutants, histopathology after HE staining revealed a destroyed crypt architecture, inflammation of the mucosa and submucosa with infiltration of neutrophils and lymphocytes, ulcerations and oedema [Figure 4 and Table 1]. The inflammation was symptomatically

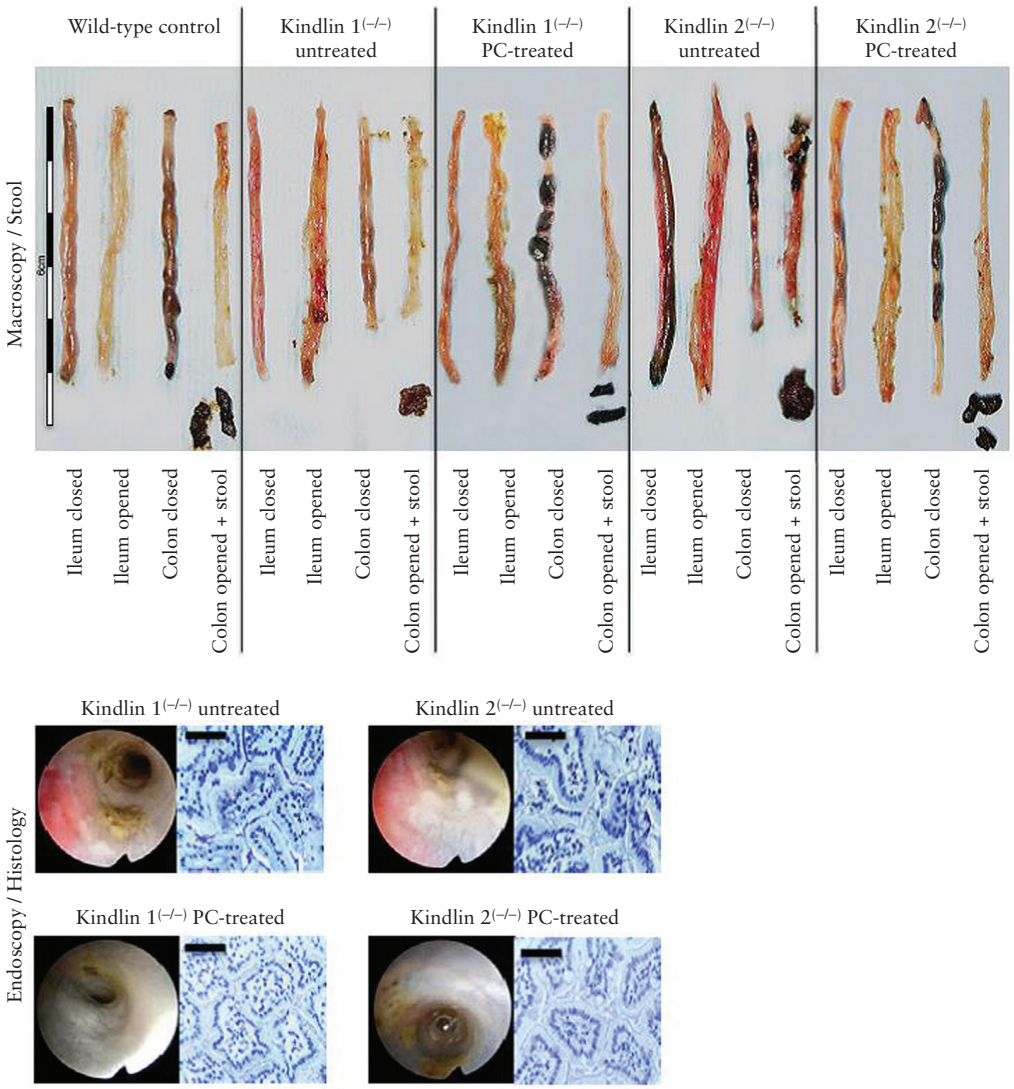

Figure 4. Macroscopic, stool, ileal endoscopic and histological features of wild-type control mice and kindlin $1^{(-/-)}$ and $2^{(-/-)}$ mice, without or with oral PC feeding. Five-centimeter sections of the terminal ileum were dissected, while the colon was entirely removed. Top: magnified sections of the closed and opened gut segments and stool samples. Bottom: endoscopic and histological features of the mutant mice, without and with PC pretreatment [scale bars = 25 µm].

Table 1. Macroscopic and histopathological evaluation of the inflammatory phenotype in kindlin $1^{(-/-)}$ and kindlin $2^{(-/-)}$ vs. wild-type mice after 3 days of tamoxifen exposure [$n = 6$]. The data are shown as the mean ± SD or the median [range].

	Wild-type	Kindlin $1^{(-/-)}$	kindlin $2^{(-/-)}$	Kindlin $1^{(-/-)}$ + PC[a]	Kindlin $2^{(-/-)}$ + PC
Macroscopic colitis score	**0 [0–1]**	**8 [8–9]**	**10 [8–11]**	**1.5 [1–3]**	**2 [1–3]**
Stool score[b]	0 [0–0]	4 [3–5]	4 [3–5]	0.5 [0–1]	2 [1–3]
Colon weight faecal content [g]	0.226 ± 0.02	0.415 ± 0.01	0.462 ± 0.01	0.309 ± 0.01	0.278 ± 0.09
Colon weight score[c]	0 [0–0]	2 [2–2]	3 [2–3]	1 [1–2]	1 [1–1]
Colon length [cm]	4.8 ± 0.3	3.7 ± 0.2	3.5 ± 0.2	4.9 ± 0.3	4.7 ± 0.4
Colon length score[d]	0 [0–1]	2 [2–3]	3 [2–3]	0 [0–0]	0.5 [0–1]
P [total score vs. wild-type]		0.003	0.003	0.011	0.007
P [total score vs. no PC]				0.003	0.003
Histopathological colitis score	**0 [0–0]**	**9 [9–10]**	**9.5 [7–10]**	**3 [1–3]**	**2 [2–4]**
Extent of inflammation[e]	0 [0–0]	2 [1–2]	2 [1–2]	0 [0–1]	0 [0–1]
Crypt architecture[f]	0 [0–0]	2 [2–2]	2 [2–2]	1 [1–2]	1 [1–2]
Hyperaemia/oedema[g]	0 [0–0]	3 [2–3]	3 [2–3]	0 [0–1]	0.5 [0–1]
Immunocyte infiltration[h]	0 [0–0]	3 [2–3]	3 [2–3]	0.5 [0–1]	0 [0–1]
P [total score vs. wild-type]		0.002	0.002	0.002	0.002
P [total score vs. no PC]				0.003	0.003
Major colitis score [macroscopic & histopathological score]	**0 [0–1]**	**18 [17–18]**	**19 [18–20]**	**4 [4–5]**	**4 [3–6]**
P [total score vs. wild-type]		0.003	0.003	0.003	0.003
P [total score vs. no PC]				0.002	0.002

[a]PC = phosphatidylcholine. [b]Stool score: 0 = normal, 1 = loosely shaped, 2 = amorphous, sticky, 3 = diarrhoea, +1 for blood. [c]Colon weight score: 0 = <10%, 1 = 10–50%, 2 = >50–100%, 3 = >100–150%, 4 = >150% weight gain compared to the wild-type mean. [d]Colon length score: 0 = <5%, 1 = 5–14%, 2 = 15–24%, 3 = 25–35%, 4 = >35% shortening compared to the wild-type mean. [e]Extent of inflammation: 0 = no inflammation, 1 = mucosa, 2 = mucosa and submucosa. [f]Crypt architecture: 0 = intact, 1 = regenerative, 2 = destroyed. [g]Hyperaemia/oedema: 0 = none, 1 = discrete, 2 = moderate, 3 = severe. [h]Immunocyte infiltration: 0 = none, 1 = discrete, 2 = moderate, 3 = severe.

abrogated by treatment with high doses of orally applied PC,[23] at 10 mg/day, by oral gavage over the 3-day period of tamoxifen exposure [Figure 4]. It was assumed that apically provided PC replenishes the empty mucus PC stores by binding to mucin 2, thus re-establishing a hydrophobic shield. The stool became solid without blood. Quantitative evaluation of inflammation[20] – including macroscopic and histopathological features – revealed a drop in the total major colitis score from 18 [17–18] and 19 [18–20] to 4 [4–5] and 4 [3–6] in kindlin $1^{(-/-)}$ and kindlin $2^{(-/-)}$ mice, respectively [$n = 6$; Table 1]. Furthermore, the calprotectin concentration in the stool fell from 1.745 ± 0.231 and 2.413 ± 0.684 mg/g stool in non-PC-treated mice to 1.341 ± 0.240 and 1.404 ± 0.374 mg/g in PC-treated kindlin $1^{(-/-)}$ and kindlin $2^{(-/-)}$ mice, respectively [$P < 0.05$ in both instances]. These values are lower than in humans, but fit the data observed in mouse UC models.[34]

3.4. Comparison of impaired mucus PC secretion in mouse mutants to human UC

Independent of their inflammatory state, UC patients have an intrinsically low mucus PC concentration and surface hydrophobicity.[9–11] Mucosal inflammation responds well to oral application of a delayed-intestinal release PC preparation that compensates for the mucus PC deficiency.[24,35,36] To study the pathophysiological link between a compromised paracellular barrier and impaired mucosal PC secretion, we investigated human colonic biopsies from patients with UC in complete remission, patients with Crohn's disease and healthy controls. Indeed, several randomly taken areas of mucosal sections exhibited in UC a defective epithelium with widened intercellular clefts, as documented in the representative electron microscopic image of Figure 5A, left. More systematically, it was shown by light microscopy in HE-stained colonic biopsies that UC patients in remission had enlarged mucosal crypts, with a crypt lumen to total crypt diameter ratio of 0.29 ± 0.04 as compared to 0.15 ± 0.04 in controls [$P < 0.001$] and 0.20 ± 0.05 in Crohn's disease patients [$P < 0.05$; Figure 5A]. This was consistent with observations in the UC mouse models and indicated a loss of TJ-mediated lateral cell attachment. For *in vivo* evaluation of PC movement to the mucus, colonic biopsies of healthy controls, patients with Crohn's disease and UC patients in complete remission were exposed to fluorescent NBD-PC [10 µm] for 1 h. Confocal laser microscopy of the frozen biopsy sections revealed in healthy controls and Crohn's disease a distinct paracellular labelling between enterocytes and fluorescence accumulation in the mucus. In contrast, patients with UC in remission showed a cuboidal shape of the enterocytes and concomitant distension of the intercellular space with impaired paracellular PC staining and reduced mucus PC fluorescence [Figure 5B, upper panel]. The resultant low luminal phospholipid content was also visible by Pearse[27] and PAS staining [Figure 5B, lower panels].

4. Discussion

It is a challenge to prove that TJ disruption is a primary event in UC and not secondary to inflammation. This is impossible to verify in the inflamed mucosa of active human UC. Accordingly, we chose patients in clinical, endoscopic and histological remission. In this instance high-resolution electron microscopy revealed a disruption of the lateral cell adhesion with widening of the intercellular space. In histological sections of the mucosa an increased ratio of lumen to total crypt diameter at a similar length position within the crypts was evident when compared to healthy controls and patients with Crohn's disease. This indicates a general widening of the crypt lumina, only in UC. Moreover, confocal laser microscopy showed that enterocytes of UC patients adopted a cuboidal shape with extended paracellular spaces, but not in healthy controls or Crohn's patients [Figure 5B, upper panel]. All these findings support the idea of a loosening of lateral TJ-mediated cell-to-cell attachment. It

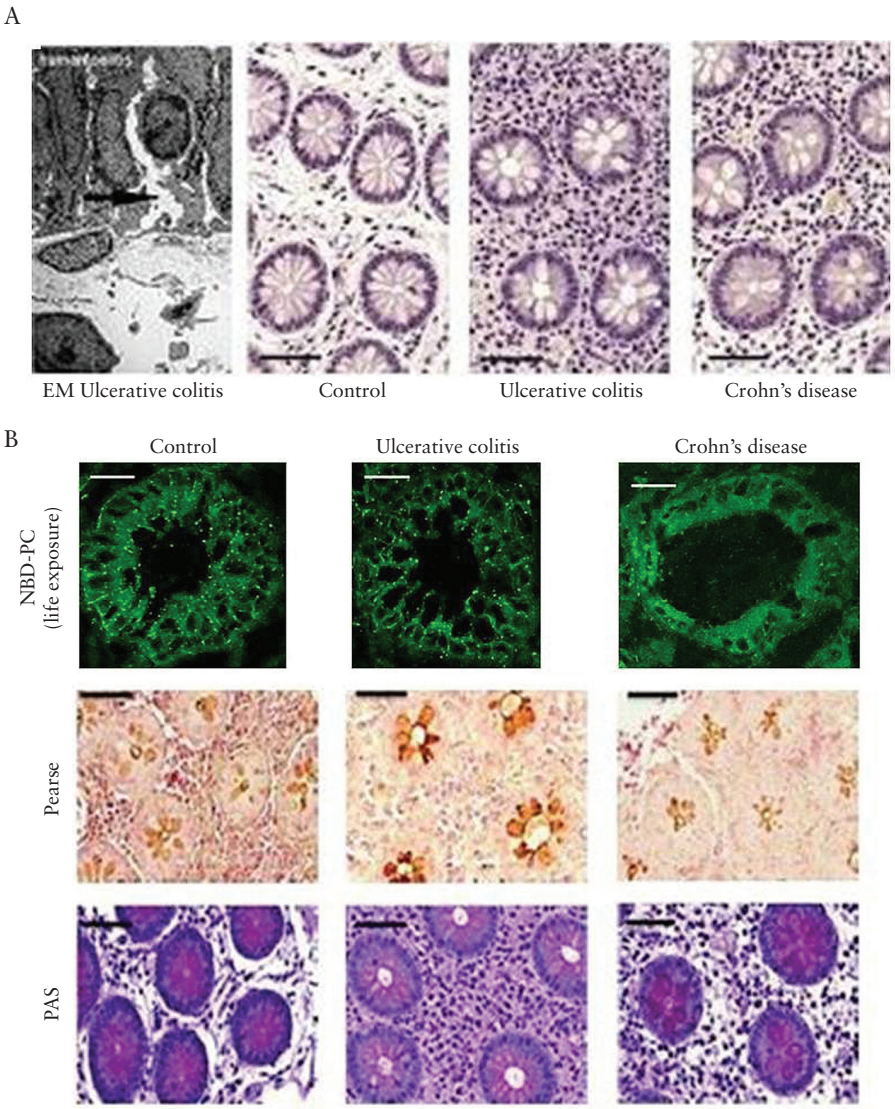

Figure 5. Widened crypts due to disturbed TJs in human UC [in remission] and consequent impairment of luminal PC accumulation. [A] Electron micrograph of a human UC specimen with epithelial disturbance [arrow shows widening of the intercellular cleft] and HE staining of non-inflamed mucosa with wider crypt lumina in UC patients than in control subjects and patients with Crohn's disease. [B] [upper panel] NBD-PC live exposure of colonic biopsies showing an impaired paracellular and mucus staining only in UC patients but not in healthy controls and patients with Crohn's disease. [lower panels] Reduced Pearse and PAS phospholipid staining of samples from UC patients in clinical remission vs. control subjects and patients with Crohn's disease [scale bars = 25 μm].

complies with the well-established feature of UC: a disturbed cryptal architecture.

The suggestion of a disturbed TJ barrier as a primary feature of UC was directly proven in mouse models with intestinal-specific deletion of kindlin 1 and 2. We used the advantage of time-programmed TJ disruption after exposure of the knockouts to tamoxifen. In both mutants the downstream cascade of operative proteins from activated integrin β1 to e-cadherin and to TJ proteins had already faded after 2 days of tamoxifen [pre-inflammatory state]. Freeze fracture electron microscopy revealed that the TJ bundles were broken. As a consequence the intercellular space was enlarged. This was systematically shown in histological sections and quantification revealed significantly distended cryptal diameters. Confocal laser microscopy verified in both mutants cuboidal enterocytes arranged in overlapping cell layers in kindlin $1^{(-/-)}$ mice due to loss of attachment to the basal membrane, whereas in kindlin $2^{(-/-)}$ mice, cuboidal enterocytes were still aligned at the basal membrane due to the predominant loss of lateral adherence. The morphological findings in the mutants and in human UC in remission were compatible.

UC has previously been described as a TJ disorder[37] and large-scale analysis of the human genome identified a gene cluster governing TJ assembly and regulation that was associated with UC development.[38] The conventional interpretation of these findings addresses increased water secretion or a leaky gut barrier at the luminal side, allowing systemic invasion of gut microbiota. However, a functional relationship between deleted TJs and defects in the luminally directed PC secretion to establish a hydrophobic shield has not been described before. The elucidation of this question was the topic of this study.

In a previous study with polarized CaCo2 cells it was shown that PC passes to the luminal side by paracellular movement across the TJ barrier.[6] Disruption of this barrier impaired the PC translocation dramatically.

To prove the finding of a unique paracellular pathway for PC, here we used wild-type mice in comparison to intestinal-specific kindlin 1 and 2 knockout mice, which were shown to reveal a broken TJ barrier. In wild-type controls a selective transport mechanism for PC to the luminal surface was operative, guaranteeing supply to the protective mucus. By 2 days of tamoxifen exposure to both mutants, TJ disruption was programmed to ensure a compromised luminal PC secretion before mucosal inflammation was evident. Under this condition TJ disruption led to a consequent low mucus PC content as a primary event for induction of a UC phenotype. The consequent cascade of events caused impaired hydrophobicity of the mucus [reduced contact angle in goniometry of the mucosal surface] and led finally to penetration of the mucosal barrier by the commensal bacterial flora.

After prolonged exposure to tamoxifen, a full-blown UC phenotype developed as a consequence of the mucosal defect. Colitis could be prevented by oral application of PC during the period of tamoxifen exposure. This is in line with previously reported clinical trials which showed that topical substitution of missing PC in mucus was beneficial to patients with UC.[24,35,36] One explanation is the observation that PC in mucus is bound to mucin 2, which is expected to be less loaded when PC secretion is diminished. Orally provided PC fills the empty PC binding sites of mucin 2 from the external [luminal] side and, thus, symptomatically re-establishes a hydrophobic mucus barrier which prevents microbiota invasion. The molecular defect of disturbed PC secretion is not corrected by this luminal exposure. The disturbed TJ barrier remains defective and as soon as the oral PC therapy is discontinued, the pathogenetic mechanism leading to microbiota invasion reoccurs.

From these data it can be concluded that the pathogenesis of UC represents a two-hit event: a broken mucosal barrier and invasion by the commensal microbiota. The intrinsic disturbance of the mucosal barrier may have a multigenetic origin which is not defined at present. The genes affected could span from TJ proteins, their cellular regulation [e.g. by integrins] and their metabolic control, as well as the CFTR and the different mucins.[39–43] TJs might also be secondarily affected, for example by inflammation due to the action of interferon gamma and tumour necrosis factor [TNF]$_\alpha$, which may aggravate or perpetuate the intrinsic mucus barrier defect.[44] Such a mechanism may explain why infections and stress in general trigger inflammatory episodes in UC and why anti-inflammatory treatment strategies targeting TNF$_\alpha$ are also effective in this regard.

The second hit concerns the mucosal invasion by colonic bacteria. Accordingly, when there is no microbiota present in the lumen, a colitis will not occur – as was shown in several genetic mouse models of IBD.[45,46] In patients with UC in remission there is a reduction of the mucus PC content to 30% of the levels in healthy controls, which is sufficient to prevent bacterial invasion. However, external triggers such as hormonal or dietary changes, stress or viral infections can precipitate inflammatory episodes. It is assumed that under those circumstances the microbiota shifts to a predominance of bacteria with higher ectophospholipase activity, which further reduces the mucus PC content below a critical threshold, thus breaking the hydrophobic barrier for other microbiota to invade. The inhibition of this phospholipase is hypothesized to prevent further thinning of the mucus PC layer and, thus, the development of colitis. This was indeed, shown by oral application of the non-absorbable phospholipase inhibitor UDCA-LPE [a bile acid–phospholipid conjugate[47]], underlining the proposed concept.[48] A complementary mode of action can be supposed by the data shown in the present study: the luminally applied PC may

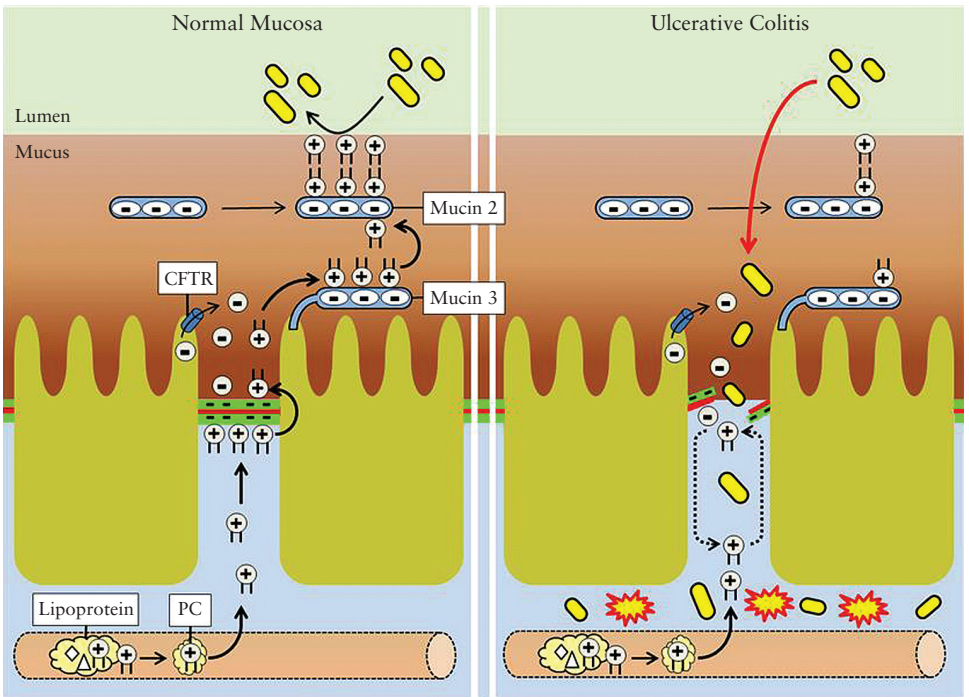

Figure 6. Scheme illustrating the proposed pathophysiological events in UC. Phosphatidylcholine [PC] in mucus establishes a hydrophobic shield against colonic microbiota. Originating from plasma lipoproteins and the segregated lipoprotein-free fraction, PC selectively accumulates in mucus via paracellular, tight junction [TJ]-dependent translocation. Transport is driven by a negative electrical gradient, with consequent binding to membrane-localized mucin 3 and an equilibrated shift to secretory mucin 2. In UC, disturbance of the TJ prevents paracellular PC secretion, resulting in a low mucus PC content, and thus reduced hydrophobicity. This predisposes the colon to microbiota invasion and mucosal inflammation.

impact on phospholipase-carrying microbiota, abrogating their pathogenic activity by saturating their aggressiveness towards to the mucus PC shield.

Taken together, our findings propose a disturbed TJ barrier as a key component in the pathogenesis of UC. The TJ construct governs a paracellular transport route for PC from systemic sources to the luminal side of the intestinal mucosa for incorporation of PC into the mucus. In UC this TJ-mediated transport of PC is genetically disrupted. It leads to a low mucus PC content, and the subsequently reduced hydrophobicity leaves the mucosal barrier vulnerable to the second devastating step: colonic microbiota invasion and consequent mucosal inflammation [Figure 6]. UC can be managed therapeutically by topical PC supplementation, which symptomatically refills the mucus PC stores, although it does not directly affect the disturbed TJ barrier. The new genetic mouse models of UC described here resemble human UC pathophysiology and are therefore useful for further experimental studies.

Funding

This work was supported in part by a grant from the Phospholipid Research Center [Heidelberg; grant-number D 10051412].

Conflict of Interest

The adult children of Wolfgang Stremmel are shareholders of Lipid Therapeutics GmbH. All other authors have declared that no financial or other conflicts of interest exist.

Acknowledgments

We thank R. Faessler [Max Planck Institute for Biochemistry, Martinsried] for providing the conditional kindlin 1 and 2 knockout mice; F. Lasitschka [Department of Pathology, Heidelberg] for biopsy preparation; D. Rohr [Department of Pharmaceutical Biology, Mainz] and R. Knittel [Department of Pathology and Neuropathology, Tübingen] for providing technical assistance with histological staining and freeze-fracture electron microscopy, respectively; W. Chamulitrat for administering PC to mice by oral gavage; and D. Hornuss for preparing the graphical scheme of Figure 6.

Author Contributions

WS: designed the study and wrote the manuscript. SS: performed the functional analyses. MS and TE: performed the histological analyses. HGS: was responsible for quantitative ESI-MS/MS phospholipid analysis. AW: performed the statistical analyses and prepared the figures. AG: assisted with the goniometry. NS: performed the endoscopies. HW: performed electron microscopy. AS: performed the FISH analysis. AM: performed confocal laser microscopy.

References

1. Podolsky DK. Inflammatory bowel disease. *N Engl J Med* 2002;**347**:417–29.
2. Kao YC, Lichtenberger LM. Phospholipid- and neutral lipid-containing organelles of rat gastroduodenal mucous cells. Possible origin of the hydrophobic mucosal lining. *Gastroenterology* 1991;**101**:7–21.
3. DeSchryver-Kecskemeti K, Eliakim R, Carroll S, Stenson WF, Moxley MA, Alpers DH. Intestinal surfactant-like material. A novel secretory product of the rat enterocyte. *J Clin Invest* 1989;**84**:1355–61.
4. Ehehalt R, Jochims C, Lehmann WD, *et al*. Evidence of luminal phosphatidylcholine secretion in rat ileum. *Biochim Biophys Acta* 2004;**1682**:63–71.
5. Stremmel W, Ehehalt R, Staffer S, *et al*. Mucosal protection by phosphatidylcholine. *Dig Dis* 2012;**30**(Suppl 3):85–91.
6. Stremmel W, Staffer S, Gan-Schreier H, Wannhoff A, Bach M, Gauss A. Phosphatidylcholine passes through lateral tight junctions for paracellular transport to the apical side of the polarized intestinal tumor cell-line CaCo2. *Biochim Biophys Acta* 2016;**1861**:1161–9.
7. Korytowski A, Abuillan W, Amadei F, *et al*. Accumulation of phosphatidylcholine on gut mucosal surface is not dominated by electrostatic interactions. *Biochim Biophys Acta* 2017;**1859**:959–65.
8. Mauch F, Bode G, Ditschuneit H, Malfertheiner P. Demonstration of a phospholipid-rich zone in the human gastric epithelium damaged by *Helicobacter pylori*. *Gastroenterology* 1993;**105**:1698–704.
9. Ehehalt R, Wagenblast J, Erben G, *et al*. Phosphatidylcholine and lysophosphatidylcholine in intestinal mucus of ulcerative colitis patients. A quantitative approach by nanoElectrospray-tandem mass spectrometry. *Scand J Gastroenterol* 2004;**39**:737–42.
10. Braun A, Treede I, Gotthardt D, *et al*. Alterations of phospholipid concentration and species composition of the intestinal mucus barrier in ulcerative colitis: a clue to pathogenesis. *Inflamm Bowel Dis* 2009;**15**:1705–20.
11. Braun A, Schönfeld U, Welsch T, *et al*. Reduced hydrophobicity of the colonic mucosal surface in ulcerative colitis as a hint at a physicochemical barrier defect. *Int J Colorectal Dis* 2011;**26**:989–98.
12. Meves A, Stremmel C, Gottschalk K, Fässler R. The Kindlin protein family: new members to the club of focal adhesion proteins. *Trends Cell Biol* 2009;**19**:504–13.
13. Rognoni E, Widmaier M, Jakobson M, *et al*. Kindlin-1 controls Wnt and TGF-β availability to regulate cutaneous stem cell proliferation. *Nat Med* 2014;**20**:350–9.
14. Montanez E, Ussar S, Schifferer M, *et al*. Kindlin-2 controls bidirectional signaling of integrins. *Genes Dev* 2008;**22**:1325–30.
15. Ussar S, Moser M, Widmaier M, *et al*. Loss of Kindlin-1 causes skin atrophy and lethal neonatal intestinal epithelial dysfunction. *PLoS Genet* 2008;**4**:e1000289.
16. Mandicourt G, Iden S, Ebnet K, Aurrand-Lions M, Imhof BA. JAM-C regulates tight junctions and integrin-mediated cell adhesion and migration. *J Biol Chem* 2007;**282**:1830–7.
17. Elias BC, Mathew S, Srichai MB, *et al*. The integrin β1 subunit regulates paracellular permeability of kidney proximal tubule cells. *J Biol Chem* 2014;**289**:8532–44.
18. Tietz S, Engelhardt B. Brain barriers: crosstalk between complex tight junctions and adherens junctions. *J Cell Biol* 2015;**209**:493–506.
19. Dawson JR, Bridges JW. Xenobiotic metabolism by isolated intestinal epithelial cells from guinea-pigs. *Biochem Pharmacol* 1979;**28**:3299–305.
20. Engel MA, Kellermann CA, Rau T, Burnat G, Hahn EG, Konturek PC. Ulcerative colitis in AKR mice is attenuated by intraperitoneally administered anandamide. *J Physiol Pharmacol* 2008;**59**:673–89.
21. Marshall W. *Clinical Biochemistry: Metabolic and Clinical Aspects*. 3rd edn. Amsterdam: Elsevier Health Science; 2014.
22. Langhorst J, Elsenbruch S, Koelzer J, Rueffer A, Michalsen A, Dobos GJ. Noninvasive markers in the assessment of intestinal inflammation in inflammatory bowel diseases: performance of fecal lactoferrin, calprotectin, and PMN-elastase, CRP, and clinical indices. *Am J Gastroenterol* 2008;**103**:162–9.
23. Kovács T, Varga G, Erces D, *et al*. Dietary phosphatidylcholine supplementation attenuates inflammatory mucosal damage in a rat model of experimental colitis. *Shock* 2012;**38**:177–85.
24. Karner M, Kocjan A, Stein J, *et al*. First multicenter study of modified release phosphatidylcholine "LT-02" in ulcerative colitis: a randomized, placebo-controlled trial in mesalazine-refractory courses. *Am J Gastroenterol* 2014;**109**:1041–51.
25. Brugger B, Erben G, Sandhoff R, Wieland FT, Lehmann WD. Quantitative analysis of biological membrane lipids at the low picomole level by nano-electrospray ionization tandem mass spectrometry. *Proc Natl Acad Sci U S A* 1997;**94**:2339–44.
26. Liebisch G, Lieser B, Rathenberg J, Drobnik W, Schmitz G. High-throughput quantification of phosphatidylcholine and sphingomyelin by electrospray ionization tandem mass spectrometry coupled with isotope correction algorithm. *Biochim Biophys Acta* 2004;**1686**:108–17.

27. Pearse AG. Copper phthalocyanins as phospholipid stains. *J Pathol Bacteriol* 1955;**70**:554–7.
28. Elsing C, Winn-Börner U, Stremmel W. Confocal analysis of hepatocellular long-chain fatty acid uptake. *Am J Physiol* 1995;**269**:G842–51.
29. Wolburg H, Liebner S, Lippoldt A. Freeze-fracture studies of cerebral endothelial tight junctions. *Methods Mol Med* 2003;**89**:51–66.
30. Swidsinski A, Göktas O, Bessler C, *et al*. Spatial organisation of microbiota in quiescent adenoiditis and tonsillitis. *J Clin Pathol* 2007;**60**:253–60.
31. Urdaci MC, Regnault B, Grimont PA. Identification by in situ hybridization of segmented filamentous bacteria in the intestine of diarrheic rainbow trout (*Oncorhynchus mykiss*). *Res Microbiol* 2001;**152**:67–73.
32. Ivanov II, Atarashi K, Manel N, *et al*. Induction of intestinal Th17 cells by segmented filamentous bacteria. *Cell* 2009;**139**:485–98.
33. Prattis S, Jurjus A. Spontaneous and transgenic rodent models of inflammatory bowel disease. *Lab Anim Res* 2015;**31**:47–68.
34. Hildebrand F, Nguyen TL, Brinkman B, *et al*. Inflammation-associated enterotypes, host genotype, cage and inter-individual effects drive gut microbiota variation in common laboratory mice. *Genome Biol* 2013;**14**:R4.
35. Stremmel W, Ehehalt R, Autschbach F, Karner M. Phosphatidylcholine for steroid-refractory chronic ulcerative colitis: a randomized trial. *Ann Intern Med* 2007;**147**:603–10.
36. Stremmel W, Merle U, Zahn A, Autschbach F, Hinz U, Ehehalt R. Retarded release phosphatidylcholine benefits patients with chronic active ulcerative colitis. *Gut* 2005;**54**:966–71.
37. Hering NA, Fromm M, Schulzke JD. Determinants of colonic barrier function in inflammatory bowel disease and potential therapeutics. *J Physiol* 2012;**590**:1035–44.
38. McCole DF. IBD candidate genes and intestinal barrier regulation. *Inflamm Bowel Dis* 2014;**20**:1829–49.
39. Quinton PM. Role of epithelial HCO_3^- transport in mucin secretion: lessons from cystic fibrosis. *Am J Physiol Cell Physiol* 2010;**299**:C1222–33.
40. Sheng YH, Hasnain SZ, Florin TH, McGuckin MA. Mucins in inflammatory bowel diseases and colorectal cancer. *J Gastroenterol Hepatol* 2012;**27**:28–38.
41. Su L, Nalle SC, Shen L, *et al*. TNFR2 activates MLCK-dependent tight junction dysregulation to cause apoptosis-mediated barrier loss and experimental colitis. *Gastroenterology* 2013;**145**:407–15.
42. Petersson J, Schreiber O, Hansson GC, *et al*. Importance and regulation of the colonic mucus barrier in a mouse model of colitis. *Am J Physiol Gastrointest Liver Physiol* 2011;**300**:G327–33.
43. Dorofeyev AE, Vasilenko IV, Rassokhina OA, Kondratiuk RB. Mucosal barrier in ulcerative colitis and Crohn's disease. *Gastroenterol Res Pract* 2013;**2013**:431231.
44. Ye D, Ma I, Ma TY. Molecular mechanism of tumor necrosis factor-alpha modulation of intestinal epithelial tight junction barrier. *Am J Physiol Gastrointest Liver Physiol* 2006;**290**:G496–504.
45. Dianda L, Hanby AM, Wright NA, Sebesteny A, Hayday AC, Owen MJ. T cell receptor-alpha beta-deficient mice fail to develop colitis in the absence of a microbial environment. *Am J Pathol* 1997;**150**:91–7.
46. Sellon RK, Tonkonogy S, Schultz M, *et al*. Resident enteric bacteria are necessary for development of spontaneous colitis and immune system activation in interleukin-10-deficient mice. *Infect Immun* 1998;**66**:5224–31.
47. Stremmel W, Staffer S, Wannhoff A, Pathil A, Chamulitrat W. Plasma membrane phospholipase A2 controls hepatocellular fatty acid uptake and is responsive to pharmacological modulation: implications for nonalcoholic steatohepatitis. *FASEB J* 2014;**28**:3159–70.
48. Stremmel W, Staffer S, Stuhrmann N, *et al*. Suppression of phospholipase a2 of intestinal microbiota by the phospholipid bile acid conjugate ursodeoxycholate-lysophosphatidyl-ethanolamide ameliorates mucosal inflammation in a genetic mouse model of ulcerative colitis. *J Crohns Colitis* 2017;**11**(suppl 1):98.